17th World Conference on Earthquake Engineering, 17WCEE
Sendai, Japan - September 13th to 18th 2020

Experimental Study on Seismic Performance of Coupling Beams Using Engineered Cementitious Composites

Z.Y. Zhang [1], R. Ding[2] , J.S. Fan[3], X.W. Hu[4]

[1] *PhD Candidate, Tsinghua University, 15516026377@163.com*
[2] *Assistant Professor, Tsinghua University, dingran@mail.tsinghua.edu.cn*
[3] *Professor, Tsinghua University, fanjsh@mail.tsinghua.edu.cn*
[4] *PhD Candidate, Tsinghua University, 903785345@qq.com*

Abstract

In a coupled-wall structure, the coupling beam is the key component for energy dissipation during an earthquake. Among all kinds of coupling beams, reinforced concrete (RC) coupling beams are the most basic form. An approach to improving the seismic performance of RC coupling beams is to use engineered cementitious composites (ECC) instead of normal concrete. Compared with normal concrete, ECC exhibits superior characteristics including tension strain-hardening and multi-cracking properties. However, there have been just a few studies about ECC coupling beams, causing the lack of understanding of the seismic behaviour. More importantly, there haven't been a precise formula that can predict the shear strength of ECC coupling beams and thus can guide the design in engineering, which have a negative effect on the application of this promising material. In this study, eight large-scale ECC coupling beam specimens with different aspect ratios, transverse and diagonal reinforcement ratios were fabricated and cyclically tested. As comparative specimens, two diagonally RC specimens are also tested. To ensure construction quality and efficiency, the ECC coupling beams were precast. Two weeks later, both the upper and lower RC end blocks were cast. The seismic performance of coupling beams is thoroughly investigated. Besides, it is worth noting that the axial elongation restraint was specially applied to the coupling beam specimens to simulate the real boundary conditions in a coupled wall structure and the axial force in the beam was measured. Finally, considering the contribution of ECC, transverse and diagonal reinforcement to shear strength, a shear strength equation is proposed based on the analysis of nineteen specimens collected from the literature and this study. The test results demonstrate that ECC coupling beams with a hybrid reinforcement layout exhibit superior seismic performance, which is a recommended choice to balance both the seismic and construction performance. It is strongly recommended that axial force should be considered in the strength prediction of coupling beams, with a 10% axial force ratio suggested for design. The proposed formula is verified and can give precise prediction for the bearing capacity of ECC coupling beams.

Keywords: Coupling Beam; Engineered cementitious composites; Hybrid layout; Axial force; Shear strength

1. Introduction

In a coupled wall structure, the coupling beam is the key component for energy dissipation during the earthquake. Among all kinds of coupling beams, the conventionally reinforced concrete (RC) coupling beam is the most basic and extensively used. However, conventionally RC coupling beams are prone to brittle failure under strong seismic excitations, which leads to unsatisfied ductility and dissipated energy. In order to improve the seismic performance of coupling beams, diagonally RC coupling beams were developed by Paulay and Binney [1], which show stronger energy dissipation capacity and larger ultimate deformation. Despite the advantages mentioned above, construction difficulties of the diagonally RC coupling beam significantly hinder its wide application. Although the ACI 318-14 code [2] provides a new kind of confinement option for diagonally RC coupling beams, the fabrication process is still complicated. Lim et al. [3] proposed a hybrid layout by combining the conventional beam detailing with the benefit of presence of proper diagonal bars, which was proved to be a good alternative to ease construction difficulty by reducing the amount of diagonal reinforcement while maintaining a sufficient shear capacity.

Besides the various reinforcement layout, another approach to improve the seismic performance of conventionally RC coupling beams is applying new types of cement-based materials instead of normal concrete. Engineered cementitious composites (ECC) is one of the representatives, which exhibits superior characteristics including tension strain-hardening and multi-cracking.

Several studies related to ECC coupling beams have been conducted. It is demonstrated from the experimental results that ECC can partially replace the transverse reinforcement and help the coupling beam dissipate more energy with slower stiffness degradation under reversed cyclic load [4-8,11]. In addition, ECC is effective in controlling the crack width and reducing the shear deformation compared with RC coupling beam [9-10].

However, the test database for the ECC coupling beam is still very small. In addition, the contribution of ECC, stirrups and diagonal bars to the shear capacity is not clear, thus leading to no formula that can precisely predict the shear capacity.

In order to enrich the test database for ECC coupling beam and quantitatively reveal the shear contribution of different components, six conventional and two hybrid ECC coupling beam specimens with different amount of transverse and diagonal reinforcement were tested in this study. As comparative specimens, two diagonally RC specimens were also tested. The aspect ratios of specimens are 2.0 and 3.0, respectively. The seismic performance of coupling beams is thoroughly investigated. Then a shear strength formula is proposed based on the analysis of all ECC coupling beams that can be collected from both in this study and in other literature. It is worth noting that the axial elongation restraint was specially applied to the coupling beam specimens to simulate the real boundary conditions in a coupled wall structure. Based on the results, the influence of axial force on shear strength of ECC coupling beams is further considered.

The main variables of the test specimens are the aspect ratio, reinforcement layout and transverse reinforcement ratio in the midspan region, as summarized in Table 1. The dimensions and reinforcement details of the typical coupling beam specimens are shown in Fig. 1.

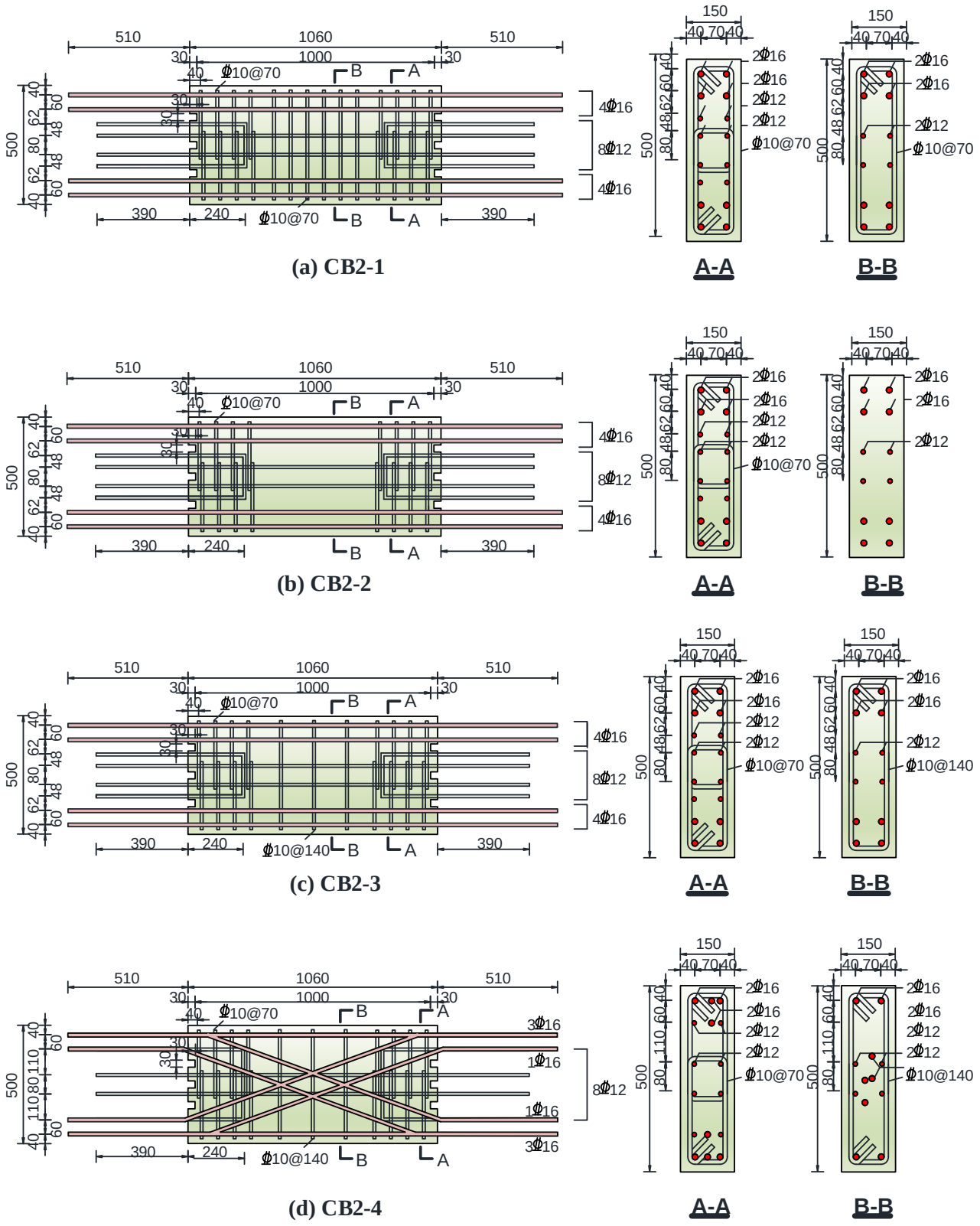

Fig. 1 – Dimensions and reinforcement details of (a) CB2-1(b) CB2-2 (c) CB2-3 and (d) CB2-4

Table 1 – Design parameters of coupling beam specimens (unit: mm)

Specimen	Materials	Width *b*	Height *h*	Span l_n	Longitudinal reinforcement	Midspan transverse reinforcement	Diagonal reinforcement
CB2-1	ECC	150	500	1000	4D16	2D10@70	
CB2-2	ECC	150	500	1000	4D16	-	
CB2-3	ECC	150	500	1000	4D16	2D10@140	
CB2-4	ECC	150	500	1000	2D16	2D10@140	2D16
CB2-5	Concrete	150	500	1000	2D16	2D10@140	2D16
CB3-1	ECC	150	333	1000	3D18	2D10@70	
CB3-2	ECC	150	333	1000	3D18	-	
CB3-3	ECC	150	333	1000	3D18	2D10@140	
CB3-4	ECC	150	333	1000	2D18	2D10@140	1D18
CB3-5	Concrete	150	333	1000	2D18	2D10@140	1D18

The cylindrical compressive strengths of normal concrete and ECC were 42.2 MPa and 54.2 MPa, respectively. The yield strengths of the rebar with the diameter of 10 mm, 12 mm, 16 mm and 18 mm were 398.6 MPa, 457.2 MPa, 449.9 MPa and 460.4 MPa, respectively.

The test setup is shown in Fig. 2. Two actuators were connected to both the north and south ends of the upper end block. When the upper end block moved towards the south direction, only the south actuator applied the pulling force while the north actuator applied no force, which can effectively prevent the out-of-plane displacement of the specimens. The two vertical struts on each side of the coupling beam were placed to apply a certain degree of axial constraint to the coupling beams. Load cells were installed in each strut to measure the corresponding axial force.

Fig. 2 – Test setup for the coupling beam specimens

2. Experimental results and analysis

When the upper end block was moving south, the displacement and force are defined positive.

2.1 Observed phenomena

For concrete specimen **CB2-5**, the first diagonal crack at a distance of 300 mm from the lower end block and flexural crack at the lower left corner were observed at the load of +100 kN (0.18 P_{ult}). At the load of +192 kN (0.35 P_{ult}), the transverse reinforcement in the midspan region yielded. When loaded to -240 kN (0.42 P_{ult}), the maximum diagonal crack width crack width reached 0.30 mm. At the same time the maximum flexural crack width also reached 0.20 mm. At the load of +298 kN (0.55 P_{ult}) and -355 kN (0.62 P_{ult}), the longitudinal reinforcement and the diagonal reinforcement yielded, respectively. When loaded to -520 kN (0.91 P_{ult}), the transverse reinforcement in the plastic hinge region also yielded. Due to the contribution of ECC, the crack width and strain in the transverse and diagonal reinforcement of ECC specimen **CB2-4** developed more slowly. When loaded to the first cycle of 3.00% drift ratio, the specimen **CB2-5** was divided into two parts. As a result, the coupling beam began to lose its shear capacity. When loaded to the first cycle of -3.00% drift ratio, the beam was divided into more pieces, companying with the crushing of concrete near the main diagonal cracks, as shown in Fig. 3e. By contrast, the main crack of ECC specimen **CB2-4** did not become wider obviously until the second cycle of -5.00% drift ratio. At that time the ECC near the lower left end block was crushed, as shown in Fig. 3d. The specimen **CB2-5** underwent typical shear tension failure mode while **CB2-4** underwent shear compression failure.

The typical failure mode and cracking behavior of other specimens are not described in detail for simplicity. The failure modes of all the ten specimens can be seen in Fig. 3.

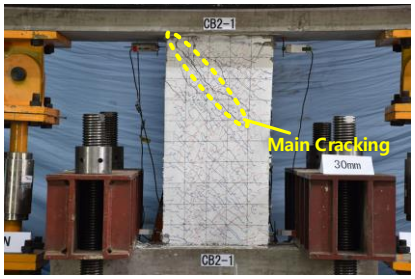

(a) CB2-1

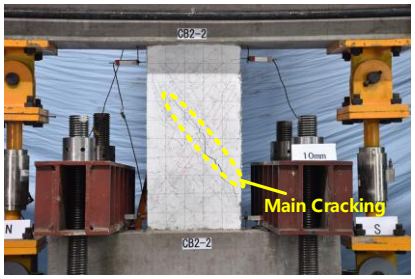

(b)CB2-2

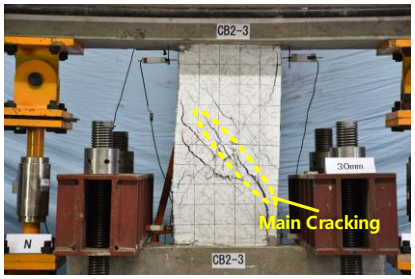

(c) CB2-3

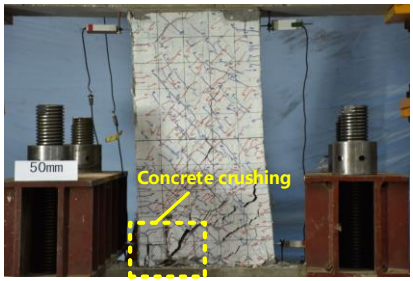

(d)CB2-4

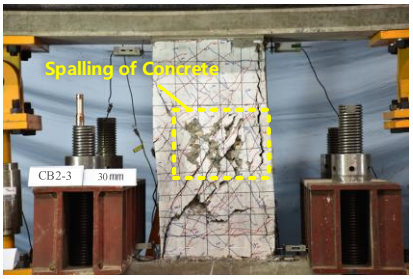

(e) CB2-5

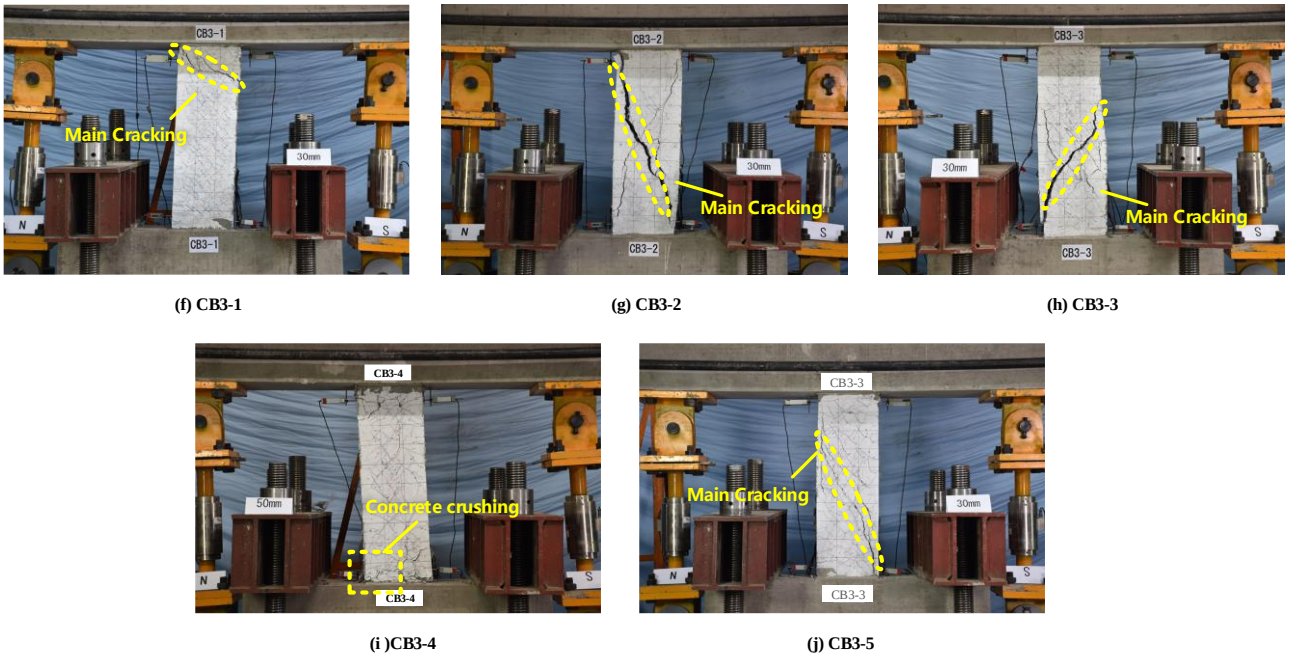

(f) CB3-1 **(g) CB3-2** **(h) CB3-3**

(i)CB3-4 **(j) CB3-5**

Fig. 3 – Failure modes of (a) CB2-1 (b) CB2-2 (c) CB2-3 (d) CB2-4 (e) CB2-5 (f) CB3-1 (g) CB3-2 (h) CB3-3 (i) CB3-4 and (j) CB3-5

2.2 Load–displacement curve

Specimen **CB2-1** exhibited a relatively stable hysteretic response. At the initial stage no obvious yield point occurred and the pinching effect isn't obvious. The drift ratio corresponding to the maximum shear force is 1.96% (-2.52%). After that, the pinching effect were observed because when the displacement returned to zero, the wide flexure-shear diagonal crack didn't close completely. Then at the next displacement level of 3.00%, the shear strength decreased by 12% and 27% in the positive direction and negative direction, respectively. Then at the drift ratio of 4.00%, there is a sudden drop with the phenomenon of shear compression failure. Considering the coupling beam is under the compression which is unfavorable for the ductility, the result is still satisfactory.

As for specimen **CB2-3**, the performance before the maximum shear force is just the same with CB2-1. Because of insufficient transverse reinforcement, the shear strength is lower and the hysteretic response is less stable due to the shear tension failure after the maximum shear force, demonstrating that the transverse reinforcement in the midspan region is still necessary for the coupling beam.

A more obvious example is specimen **CB2-2** which doesn't have any transverse reinforcement in the midspan region. It exhibited low shear strength and poor ductility. After reaching the maximum shear strength with the drift ratio of 1.02% (-0.80%), a sudden drop could be seen in both directions accompanying with shear tension failure.

For hybrid-layout specimen **CB2-5** made of concrete, when loaded to the drift ratio of +2.63% (-1.57%), the load reached the maximum. Then when loaded to the second cycle of 3.00% drift ratio, the shear strength decreased by as far as 77.6%. The specimen also had poor ductility because of shear tension failure.

For specimen **CB2-4** with hybrid layout, the hysteretic curve is the fullest among specimens with the aspect ratio of 2.0. The shear force reached the maximum at the drift ratio of 3.37% (-4.02%), before which the shear capacity of other specimens had decreased to less than 50% of the maximum shear force. Even when loaded to the drift ratio of 6.00%, the shear strength only decreased to 49.5%. From the comparison, it can be seen that specimen CB2-4 with hybrid layout exhibited extraordinary performance including higher shear

capacity and better ductility. The plumper curve of the specimen CB2-4 indicates the larger energy dissipation capacity than the other specimens.

As can be seen in Fig. 4f–4j, the characteristics of the load–displacement curves for the CB3 specimens with an aspect ratio of 3.0 are very similar to those of the CB2 specimens with an aspect ratio of 2.0 discussed above, so they aren't discussed in detail for simplicity.

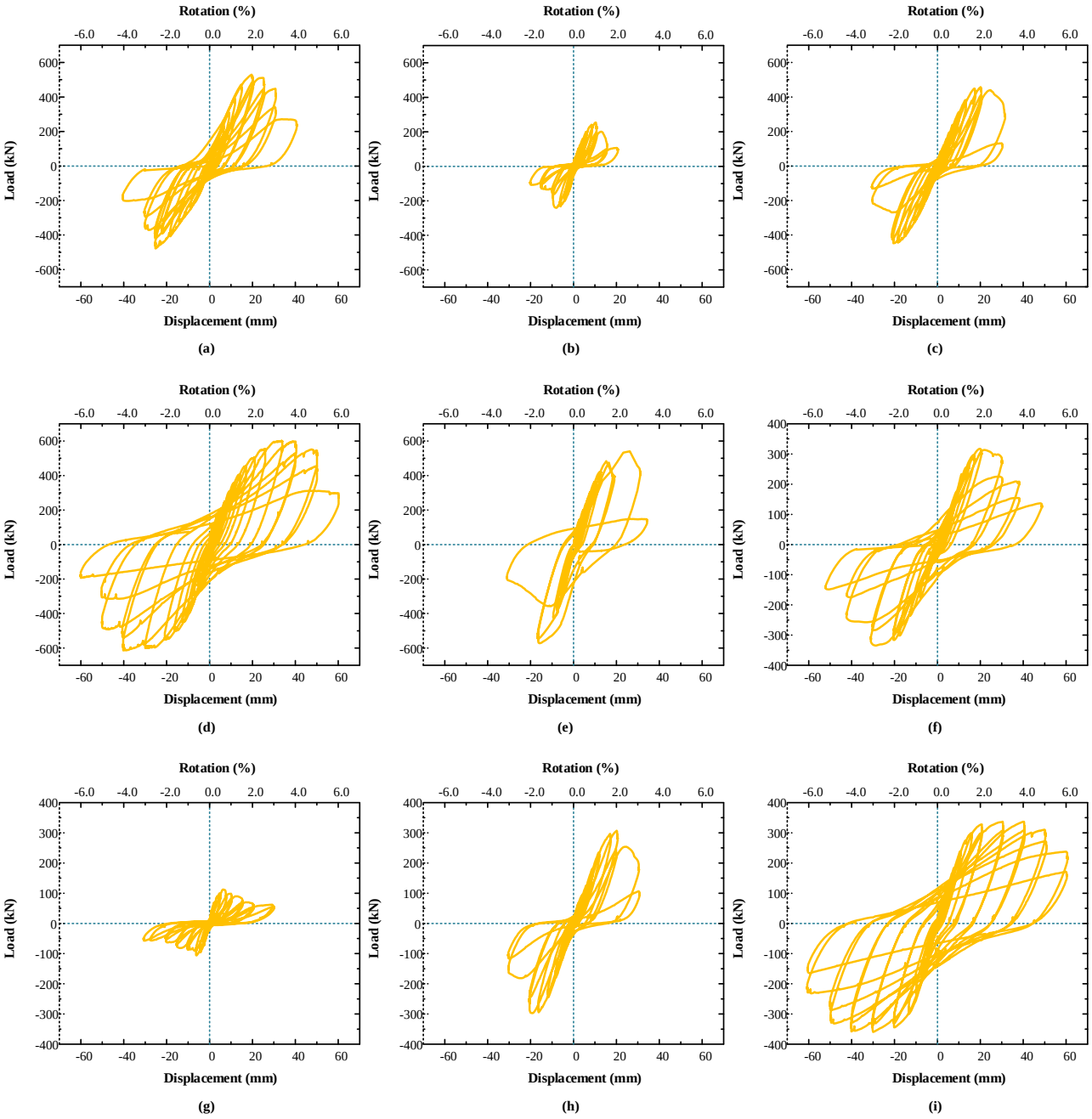

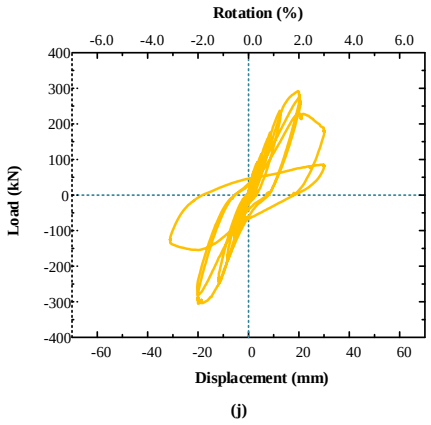

Fig. 4 – Load–displacement curves of (a) CB2-1 (b) CB2-2 (c) CB2-3 (d) CB2-4 (e) CB2-5 (f) CB3-1 (g) CB3-2 (h) CB3-3 (i) CB3-4 and (j) CB3-5

3. Monitoring of axial force

According to Kwan at al. [12], the axial elongation will occur in the coupling beams without axial restraint. However, Lequesne et al. [10] pointed out that coupling beams with axial restraint was more realistic. As a result, a certain degree of axial restraint was applied in this investigation. Therefore, there exists axial pressure force in the coupling beams. The maximum shear force P_{ult}, the maximum axial force N_{ult}, and the maximum axial force ratio are summarized in Table 2. It can be found that the largest axial force ratio is 14.2%, exceeding the lower limit in the ACI 318-14 code [2] to neglect effects of axial force in strength calculations. Whether considering the axial force or not has a great influence on the calculated strength. The calculated strength considering the axial force is 22% larger than the calculated strength without the axial force for the specimen CB2-4. As a result, for the design of the coupling beams, considering 10% axial force ratio is suggested.

Table 2 – Summary of measured axial force in the coupling beam specimens

Specimen	Ultimate shear force P_{ult} (kN)	Maximum axial force N_{ult} (kN)	Maximum axial force ratio
CB2-1	529.7	360.0	0.089
CB2-2	254.0	89.2	0.022
CB2-3	457.2	218.6	0.054
CB2-4	614.5	545.7	0.134
CB2-5	572.6	323.2	0.102
CB3-1	335.9	255.7	0.094
CB3-2	112.6	168.4	0.062
CB3-3	307.1	132.1	0.049
CB3-4	359.6	385.7	0.142
CB3-5	305.4	201.7	0.096

4. Proposed formula for the ultimate capacity of coupling beams

According to Ding et al. [13], there are four failure modes for coupling beams: shear tension, shear compression, shear sliding and flexure. With enough U-shaped bars and shear keys at the end of the coupling beams, shear sliding failure mode can be prevented. If the amount of the transverse reinforcement is relatively low compared with the longitudinal reinforcement, the failure will occur in the midspan of the coupling beam, which is the shear tension failure mode. On the contrary, if the amount of the transverse reinforcement is relatively high, the failure will occur at the plastic hinge region, which is the flexure failure mode or the shear compression failure mode. For the latter situation, the bearing capacity is determined by

the flexure strength which can be accurately calculated by the strip method. For the former situation, the bearing capacity is determined by the shear strength of the beam. There have been several models to predict the shear strength of RC coupling beams, including formulas from ACI 318-14 [2], FEMA 306 [14] and so on. In these formulas, the contribution of concrete, transverse and diagonal reinforcement is considered separately. However, there is no formula that can accurately predict the shear strength for ECC coupling beams. The main reason is the different contribution between concrete and ECC. Considering that the shear mechanisms of RC coupling beams and ECC coupling beams are the identical, the form of the formula to predict the shear strength of ECC coupling beams should be the same as the formula of RC coupling beams. Ding at al. [13] pointed out that formula from the ACI 318-14 code [2] gives the best prediction for RC coupling beams. And according to Lim at al. [3], shear strength contributed by the diagonal reinforcement is given by Eq. (1):

$$V_d = (1.0+1.1)A_{sd}f_{sd}\sin\alpha \tag{1}$$

where A_{vd}, f_y and α denotes the area, yield stress and the inclination angle of one group of diagonal reinforcement, respectively. The coefficient 1.1 is decided by considering the strain hardening of diagonal reinforcement under tension. Therefore, the predicted shear strength V_s can be written as Eq. (2):

$$V_{us} = \frac{A_{sv}f_{sv}d}{s} + k\sqrt{f_c'}bd + (1.0+1.1)A_{sd}f_{sd}\sin\alpha \tag{2}$$

where A_{sv}, f_{sv} and s denotes the area, yield stress and space of the transverse reinforcement, respectively; b and d denotes the width and effective height of the section, respectively; f_c' denotes cylinder concrete compressive strength; k denotes the coefficient depending on shear span.

In order to propose an accurate formula to predict the shear strength, ECC coupling beam test specimens without steel fiber are collected and listed in Table 3. The maximum axial force N_{ult}, the ultimate load based on test data V_{test}, the flexure strength without considering the axial force V_{m1}, the flexure strength considering the axial force V_{m2}, the shear strength proposed in this article V_s and the predicted bearing strength V_{pre}, which is the minimum value between V_{m2} and V_s are summarized. According to the data collected both from this study and other investigation, k of ECC tends to linearly decrease with the increase in l_n/h. Therefore, the following formula is proposed:

$$k = -0.14\frac{l_n}{h} + 0.82 \tag{4}$$

Table 3 – Database of ECC coupling beam test specimens

Author	Name	N_{ult} (kN)	V_{test} (kN)	V_{m1}(kN)	V_{m2} (kN)	V_s(kN)	V_{pre}(kN)	V_{pre}/ V_{test}
This Article	CB2-1	360.0	529.7	463.6	546.6	686.2	546.6	1.032
	CB2-2	89.2	254.0	463.6	484.4	274.4	274.4	1.080
	CB2-3	218.6	457.2	463.6	516.9	480.3	480.3	1.051
	CB3-1	255.7	335.9	286.8	325.6	391.7	325.6	0.969
	CB3-2	168.4	112.6	286.8	312.3	129.3	129.3	1.148
	CB3-3	132.1	307.1	286.8	306.8	260.5	260.5	0.848
Han et al. [9]	FC-0-2.0	-	909.0	696.0	849.2 [a]	916.6	849.2	0.934
	FC-0.5-2.0	-	1163.0	1034.7	1151.9 [a]	1165.3	1151.9	0.990
	FC-0-3.5	-	452.0	387.6	424.6 [a]	428.1	424.6	0.939
	FC-0.5-3.5	-	562.0	498.9	529.4 [a]	561.4	529.4	0.942
Canbolat et al.[6]	specimen2	-	600.0	767.7	1185.1 [a]	554.9	554.9	0.925
	specimen3	-	800.0	791.3	1179.4 [a]	778.3	778.3	0.973
Shin at al. [7]	1cf2y	884	491.0	351.8	482.0	488.5	482.0	0.982
	1df2y	1009	533.0	450.3	483.7	735.4	483.7	0.907
Che [11]	CB-3	0	510.4	810.4	-	472.6	472.6	0.977

CB-4	0	513.0	864.7	-	501.2	501.2	1.074
CB-5	0	560.0	926.1	-	601.7	601.7	0.979

[a] *The flexure strength is calculated considering 10% axial force ratio.*

The last column in Table 3 shows the accuracy of the predicted capacity for all 19 specimens. It can be seen that the formula proposed in this study provides satisfactory prediction of the shear strength of ECC coupling beams if shear–tension failure mode occurs. Besides, the calculated flexure strength considering the axial force correlates better with test data if shear compression failure mode occurred. As a result, the axial force in the coupling beams should be seriously considered.

5. Conclusions

In order to quantitatively evaluate the influence of different components on the seismic performance and shear strength of ECC coupling beams, specimens with different aspect ratios, transverse and diagonal reinforcement were fabricated and tested. The following conclusions can be drawn on the basis of the findings from the coupling beam tests:

(1) ECC specimens with hybrid layout exhibited extraordinary performance including higher shear capacity, better ductility and energy dissipation capacity. Therefore, the hybrid layout is a considerable choice to balance both the seismic performance and construction performance.

(2) According to the results, the largest axial force ratio of these specimens is 14.2%, exceeding the lower limit in the ACI 318-14 code [2] to neglect effects of axial force in strength calculations. Whether considering the axial force or not has a great influence on the calculated strength. Therefore, it is highly recommended that 10% axial force ratio should be considered if axial force is unknown.

(3) A new formula for calculating the shear strength of the ECC coupling beam if shear tension failure occurred was proposed in this paper. The calculated values were in good agreement with test results not only from this investigation, but also from other literatures.

6. References

[1] Paulay T, Binney JR. Diagonally reinforced coupling beams of shear walls. ACI Spec. Publ. 1974; 42: 579-598.

[2] ACI 318-14. Building code requirements for structural concrete (ACI 318-14) and commentary/reported by ACI Committee 318. Farmington Hills, Mich.: American Concrete Institute; 2014.

[3] Lim E, Hwang SJ, Wang TW, Chang YH. An investigation on the seismic behavior of deep reinforced concrete coupling beams. ACI Struct J 2016; 113(2): 217-226.

[4] Setkit M. Seismic behavior of slender coupling beams constructed with high-performance fiber-reinforced concrete. Ph.D. Dissertation. University of Michigan; 2012.

[5] Lim E, Hwang SJ, Cheng CH, Lin PY. Cyclic tests of reinforced concrete coupling beam with intermediate span-depth ratio. ACI Struct J 2016; 113(3): 515-524.

[6] Canbolat BA, Parra-Montesinos GJ, Wight JK. Experimental study on seismic behavior of high-performance fiber-reinforced cement composite coupling beams. ACI Struct J 2005;102(1): 159–166.

[7] Shin M, Gwon SW, Lee K, Han SW, et al. Effectiveness of high performance fiber-reinforced cement composites in slender coupling beams. Constr Build Mater 2014; 68: 476–490.

[8] Park WS, Yun HD. Seismic performance of pseudo strain-hardening cementitious composite coupling beams with different reinforcement details. Compos Part B-Eng 2011; 42(6): 1427–1445.

[9] Han SW, Lee CS, Kwon HW, et al. Behaviour of fibre-reinforced beams with diagonal reinforcement. Mag Concrete Res 2015; 67(24); 1287–1300.

[10] Lequesne RD, Parra-Montesinos GJ, Wight JK. Seismic behavior and detailing of high-performance fiber-reinforced concrete coupling beams and coupled wall systems. J Struct Eng 2012; 139(8): 1362–1370.

[11] Che JL. Research on seismic performance and design method of FRC diagonally reinforced coupling beams and coupled shear walls. Dissertation. Xi'an University of Architecture and Technology, China; 2013. (in Chinese)

[12] Kwan AKH, Zhao ZZ. Cyclic behaviour of deep reinforced concrete coupling beams. Proc. ICE, Struct & Build, 2002; 152(3): 283-293.

[13] Ding R, Tao MX, Nie JG, et al. Shear deformation and sliding-based fiber beam-column model for seismic analysis of reinforced concrete coupling beams. J Struct Eng 2016; 142(7): 04016032.

[14] Federal Emergency Management Agency (FEMA) 306, Evaluation of earthquake damaged concrete and masonry wall buildings—Basic procedures manual. Washington, DC.: Applied Technology Council; 1999.

